A Modeling Study on Performance of a CNOT Gate Devices based on Electrode-driven Si DQD Structures

Hoon Ryu[§*] and Ji-Hoon Kang[§]
[§]Korea Institute of Science and Technology Information (KISTI), Daejeon 34141, Republic of Korea
[*]Electronic mail: elec1020@kisti.re.kr

***Abstract*— Behaviors of quantum bits (qubits) encoded to electron spins in silicon double quantum dot (Si DQD) systems are examined with a multi-scale modeling approach that combines electronic structure simulations and Thoas-Fermi calculations. Covering the full-stack functionality of Si DQD devices from electrode-driven charge controls to logic operations, we investigate the sensitivity of exchange interaction between two initialized qubits and its effect on the fidelity of controlled-NOT gate operations to understand the experimental reported feature. This preliminary work not only presents a theoretical clue for understanding the major control factors for the gate fidelity, but opens the possibility for further exploration of the engineering details of qubit logic gate devices that is hard to be uncovered with experiments due to the time and the expense.**

I. Introduction

Silicon(Si) has obtained attention for universal quantum gate designs due to its strong potential of easy integration with classical control hardwares using industry-standard fabrication processes. Recently, experimentalists reported a successful implementation of the controlled-NOT (CNOT) gate based on electrode-driven silicon (Si) double quantum dot (DQD) structures [1] with the theoretical foundation presented by Russ *et al.* [2]. Detailed design guidelines for Si DQD qubit gates are not still clear due to the lack of modelling studies that escalate device simulations to the level of logic gate operations. In this preliminary work, we study the effects of physical design factors of Si DQD structures on CNOT operations with a full-stack modeling approach that covers device simulations as well as corresponding time responses of spin-qubits.

II. Methods

Figure 1(a) shows the simulated DQD structure, which is 2D as the dimension along [001] direction is assumed to be very long as the experimentally reported structure is [1]. At T=1.5K, the bias-dependent electrostatic of Si DQD is simulated with Thomas-Fermi (TF) model [3] assuming the Fermi-energy (E_F) of source-drain electrodes is 0. The QD region near the middle Si layer that confines electrons is simulated with an single-band effective mass model [4] to correct TF-driven charges. A DC magnetic field is applied along [010] direction (B_Y) with a maximal magnitude of 300mT and a $\sim 40\mu\mathrm{T/nm}$ gradient along [100] direction, to mimic the distribution generated by a cobalt miromagnet [5]. Frequency and magnitude of an AC magnetic field that is applied along [100] direction (B_X) are used as control variables. Time responses of spin-qubits are simulated with the Heisenberg Hamiltonian of two neighboring spins in a varying magnetic field [2].

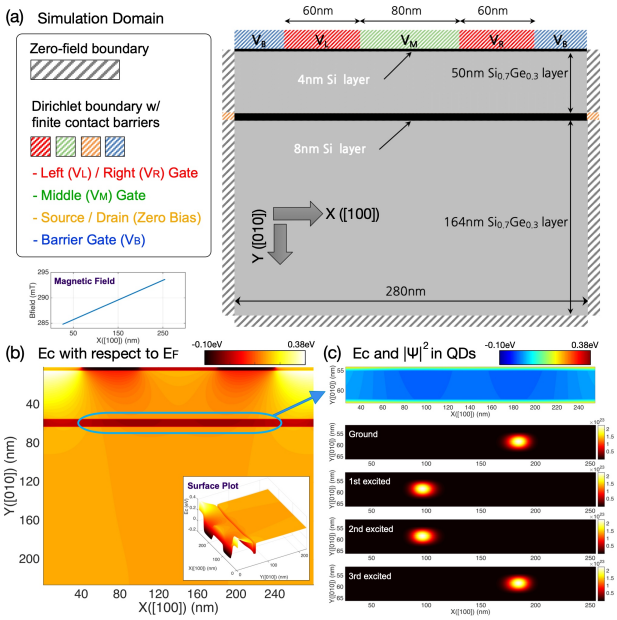

Fig. 1. **Si DQD device and electronic structures.** (a) A 2D simulation domain describing a Si double quantum dot (DQD) structure that is assumed be very long along [001]direction. Quantum confinement along [100] (X) direction is formed by controlling biases applied on top electrodes (V_L,V_M,V_R). Confinement along [010] (Y) direction is created by the conduction band offset between Si and $Si_{0.7}Ge_{0.3}$ layers. (b) Local band structure (E_C, conduction band diagram) of the DQD system when V_L = V_R = 542mV and V_M = 400mV, and (c) Electron density ($|\Psi|^2$) at the 4 lowest conduction band states. Due to the magnetic field (B_Y) gradient along X direction, Zeeman-splitting in right QD is slightly larger than the one in left QD.

III. Results and Discussion

Wavefunctions in empty DQD: Figure 2(b) shows the conduction band diagram of the Si DQD structure that are simulated with V_L = V_R = 542mV and V_M = 400mV. Due to the conduction band offset between Si and $Si_{0.7}Ge_{0.3}$ layers, vertical confinement (along [010] direction) is created near the middle Si layer and lateral confinement (along [100]) is driven by biases of the three electrodes. Though QDs are empty in this bias-condition, it is still possible to explore the confinement-driven energy states.

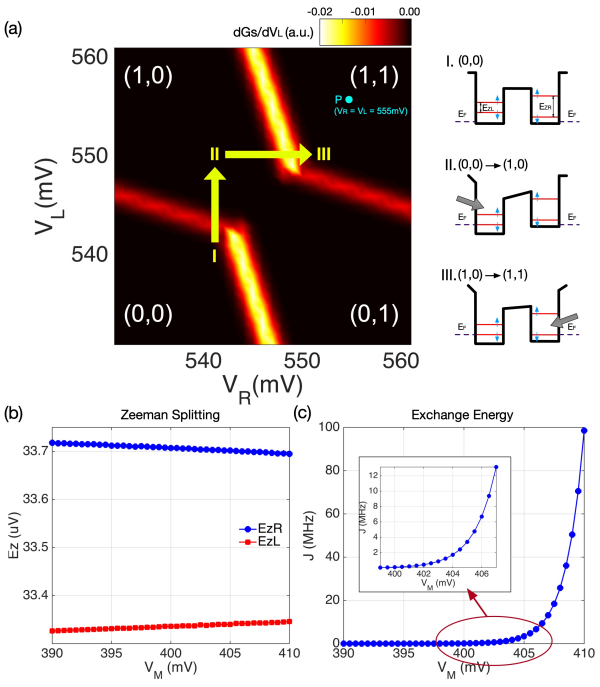

Fig. 2. **Charge and spin-qubit controllability.** (a) A charge stability diagram shown as a function of (V_L,V_R) biases (V_M is set to 400mV) The first step needed for a CNOT operation is to initialize the double quantum dot (DQD) system so both the left and right QD downspin ($|\downarrow\rangle$) state are occupied by a single electron ((1,1) region in the stability diagram). The conceptual band diagrams given in the right side explain the variation of QD potential along the path of charge transfer marked with yellow arrows in the stability diagram. (b) Zeeman-splitting of the right (EzR) and left (EzL) QD and (c) Exchange constant (J) of the two downspin states shown as a function of V_M (V_L = V_R = 555mV). ΔV_M of 20mV does not drive remarkable changes of EzR and EzL, but J is very sensitive to V_M.

Electron densities ($|\Psi|^2$) of the 4 lowest conduction band states are given in Figure 1(c). Here, the 1st (ground) and 4th (3rd excited) state are down/upspin ($|\downarrow\rangle$/$|\uparrow\rangle$) state of the right QD, where the remaining two states are those of the left QD. Zeeman-splitting in right and left QD are calculated as 33.7μeV and 33.3μeV, respectively, and show a 0.4μeV difference due to B_Y gradient along [100] direction.

Control of charge/energy-splitting/exchange constant: A full charge stability diagram is shown in Figure 2(a) and the left arrows indicate the path of charge transfer (0.0)→(1,0)→(1,1), where the two numbers in parentheses mean the number of electrons filled in left/right QD. Corresponding variation of DQD conduction band diagram is conceptually illustrated in the right subfigures. The starting step of qubit operations is to initialize the DQD system such that the $|\downarrow\rangle$ state of each QD is filled with a single electron ($|\downarrow\rangle_L \otimes |\downarrow\rangle_R = |\downarrow\downarrow\rangle$). When V_M is set to 400mV, our results show that $V_R = V_L > 500$meV are required to perform this initialization process. Once the initialization is done, the energy-level of four 2-qubit states ($|\downarrow\downarrow\rangle$/$|\downarrow\uparrow\rangle$/$|\uparrow\downarrow\rangle$/$|\uparrow\uparrow\rangle$) is determined with Zeeman-splitting in each QD (EzR/EzL) and exchange constant

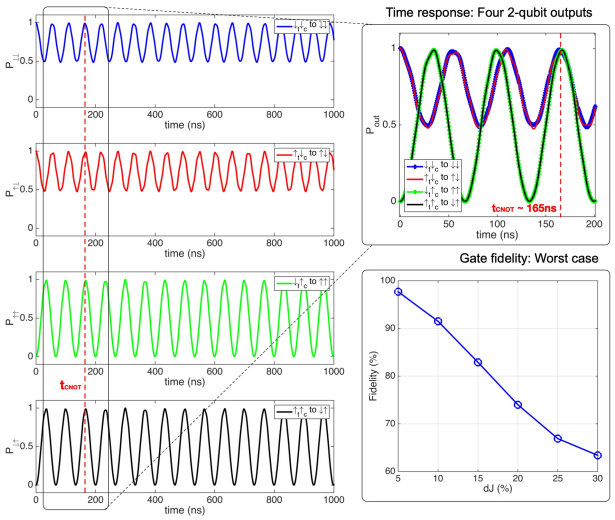

Fig. 3. **CNOT gate operation and fidelity of the worse case.** The left 4 subfigures show time responses of our DQD system against the 4 2-qubit inputs at V_L = V_R = 555mV and V_M = 407mV. Frequency of the left qubit oscillation depends on the right qubit so, oscillations in the first and last 2 subfigures have slightly different frequencies. At t_{CNOT} = 165(ns), however, the oscillations are synchronized and a CNOT operation is conducted. The zoomed-in time responses are given in the right-top subfigure. Fidelity of a CNOT gate operation strongly depends on the charge noise whose effect is considered with unexpected deviation of the exchange constant (dJ).

(J) between $|\downarrow\rangle_L$ and $|\downarrow\rangle_R$ state wavefunction. As shown in Figure 2(b), controlling V_M in a 20mV range (directly related to the barrier height between two QDs) does not drive remarkable changes of EzL and EzR. However, the sensitivity of J to ΔV_M is extremely large and ΔV_M of 10mV is large enough to increase J by a factor of 100. J is the reason why the spin-states in two QDs can be entangled. However, its strong sensitivity to control signals becomes the very issue that must be overcome to procure the stability of gate operations.

Logic operation of CNOT gate: The real-time CNOT gate operation is simulated at V_L = V_R = 555mV and V_M = 407mV, and time responses of the four 2-qubit inputs are shown in left subfigures of Figure 3, where the top and bottom two subfigures show an oscillation of the left qubit given that the right qubit is $|\downarrow\rangle$ and $|\uparrow\rangle$, respectively. Under an AC magnetic field (B_X) of ∼1mT amplitude, the oscillations have slightly different frequencies but are synchronized at ∼165ns, conducting a CNOT operation. The right-bottom subfigure in Figure 3 shows the gate fidelity as a function of unexpected deviation of J (dJ), where we observe 20% of dJ already reduces the fidelity under 80%.

IV. Conclusion

A preliminary modeling study on the controlled-NOT logic gate device based on the silicon double quantum dot structure is presented. We find that the exchange interaction between a ground-state electron in each quantum dot, which turns out to be extremely sensitive to the

bias applied to the barrier gate electrode, would become the major factor that can explain why the experimentally reported fidelity [1] is quite lower than other competitors such as 2-qubit logic gate devices based on superconductors [6] and ion traps [7].

ACKNOWLEDGMENTS

This work has been supported by the Korea Institute of Science and Technology Information (KISTI) institutional R&D program (K-20-L02-C09) and the Institute for Information & communication Technology Promotion (IITP) grant (2019-0-0003) funded by Korea government(MSIP). The NURION high performance computing resource has been extensively used for all the simulations.

REFERENCES

[1] D. M. Zajac, A. J. Sigillito, M. Russ, F. Borjans, J. M. Taylor, G. Burkard, and J. R. Petta, "Resonantly driven CNOT gate for electron spins," *Science* 359, pp. 439-442 (2018).

[2] M. Russ, D. M. Zajac, A. J. Sigillito, F. Borjans, J. M. Taylor, J. R. Petta, and G. Burkard, "High-fidelity quantum gates in Si/SiGe double quantum dots," *Physical Review B* 97, p. 085421 (2018).

[3] V. Grimalsky, L. M. Gaggero-Sager, and S. Koshevaya, "Electron spectrum of δ-doped quantum wells by the Thomas-Fermi method at finite temperatures," *Physica B: Condensed Matter* 406, pp. 2218-2223 (2011).

[4] J. Wang, A. Rahman, A Ghosh, G. Klimeck, and M. Lundstrom, "On the Validity of the Parabolic Effective-Mass Approximation for the I-V Calculation of Silicon Nanowire Transistors," *IEEE Transactions on Electron Devices* 52, pp. 1589-1595, (2005).

[5] R. Neumann and L. R. Schreiber, "Simulation of micro-magnet stray-field dynamics for spin qubit manipulation," *Journal of Applied Physics* 117, p. 193903 (2015).

[6] S. Li, A. D. Castellano, S. Wang, Y. Wu, M. Gong, Z. Yan, H. Rong, C. Zha, C. Guo, L. Sun, C. Peng, X. Zho, and J.-W. Pan, "Realisation of high-fidelity nonadiabatic CZ gates with superconducting qubits," *npj Quantum Information* 5, p. 84 (2019).

[7] T. Choi, S. Debnath, T. A. Manning, C. Figgatt, Z.-X. Gong, L.-M. Duan, and C. Monroe, "Optimal quantum control of multimode couplings between trapped ion qubits for scalable entanglement," *Physical Review Letters* 112, p. 190502 (2014).